# LIMITING PRECISION IN A SCANNING OPTICAL INTERFEROMETER

## By R. M. Hill* and C. F. Bruce*

*Summary*

An examination of the limiting precision with which a scanning optical interferometer can be pointed on a fringe peak is described. The interferometer uses photoelectric detection and it is shown that the principal noise sources limiting the accuracy of detection are the shot noise in the vacuum photocell and the photon noise from the light source.

Comparison is made with experimental results obtained on an oscillating Fabry–Perot interferometer and the agreement is reasonable. The peak precision of setting, or pointing, for the 6056 Å line of krypton 86 isotope, using silver films with a reflectance of 83%, was $2 \cdot 9 \times 10^9$ experimentally, and $3 \cdot 7 \times 10^9$ theoretically.

The scanning Fabry–Perot interferometer can be operated at near-optimum performance throughout a range of plate separations by adjusting the amplitude of scan. For the krypton radiation, the precision of setting can be within 10% of its maximum value of $1 \cdot 1 \times 10^{10}$ for dielectric films or $7 \cdot 5 \times 10^9$ for silver films, for plate separations in the range 10–100 mm.

From the limiting precision of pointing on a fringe, the limiting precisions of the measurement of small wavelength shifts and of the measurement of wavelengths have been calculated. Small wavelength shifts in the krypton radiation can be measured with a maximum precision of $6 \cdot 0 \times 10^9$ with a dielectric coated Fabry–Perot interferometer, or $1 \cdot 6 \times 10^9$ with a Michelson interferometer. The mercury green 198 isotope radiation can be measured against the krypton orange-red with a maximum precision of $2 \cdot 9 \times 10^9$ with a silver-coated Fabry–Perot interferometer, or $1 \cdot 2 \times 10^9$ with a Michelson interferometer.

## I. Introduction

The redefinition of the metre in terms of the radiation from a krypton 86 isotope lamp, and the establishment of acceptable secondary wavelength standards have emphasized the importance of accurate measurement of wavelength, and wavelength shifts due to perturbations, of various radiations.

The accuracy of measurement in this work depends essentially on the precision with which pointing on a fringe in an optical interferometer may be done. This precision has become very high for both the Michelson and Fabry–Perot interferometers through the use of photoelectric detection methods. Precision may be defined as the ratio $n/\delta n$ where $\delta n$ is the smallest detectable change in the order of interference $n$.

Terrien (1958) considered the effects of lamp fluctuations and shot noise in a photodetecting Michelson interferometer and assumed that the Johnson effect would be small compared with these noise sources. He calculated that, for a photocathode current of about $10^5$ electrons/sec, the theoretical precision was $10^9$.

* Division of Applied Physics, National Standards Laboratory, C.S.I.R.O., University Grounds, Chippendale, N.S.W.

A fundamental limit to the precision has been investigated by Hanes (1959). In this work, an analysis was made of the maximum theoretical precision in the Michelson and Fabry–Perot interferometers by assuming that the smallest detectable signal is that signal which gives an output change equal to the r.m.s. photon noise background. This gives a maximum precision in terms of the physical constants of the interferometer, the radiation, the photodetector efficiency, and a quality of setting function $Q$. The method of pointing on a fringe examined was that in which intensity measurements were made on the two flanks of the fringe for equal times, and the integrated intensities were compared. When these values were equal, the positions of observation were said to be equally spaced about the fringe peak, within the error value.

From Hanes' results, the 6056 Å line of krypton 86, using a dielectric-coated Fabry–Perot interferometer of plate diameter 40 mm and at a spacing of 50 mm, would give a limiting precision of one part in $2 \cdot 1 \times 10^{10}$.

Smith (1960) has investigated the precisions of setting attainable by three different methods in terms of the shot noise in the photocathode current. With a pressure scanning interferometer system, an experimental precision of $1 \cdot 2 \times 10^9$ was obtained in comparison with the theoretically predicted value of $5 \cdot 8 \times 10^9$.

The quality of setting factor has been recalculated for a scanning interferometer using a tuned, phase-sensitive detection system. This instrument, which can be either an oscillating-plate type, or a pressure-controlled type, is more commonly used for wavelength comparisons than the flux measurement system. A setting is made directly on the fringe peak by examining the oscillating signal from a photodetector mounted directly behind an aperture centred on the haidinger ring system. The output from the cell is passed to a synchronous detector that can be used to display a signal proportional to the displacement of the mean setting of the interferometer from the peak.

Other noise factors have been considered besides the quantum noise examined by Hanes. These arise from the shot noise and the Johnson noise imposed on the detected signal and the limitations of the photomultiplier tube. The limiting precision of a practical interferometer is shown to depend on a total noise function $\Phi$, and comparison is made between the theoretical values and experimentally determined results for the 6056 Å line of krypton 86 isotope and the 5461 Å line of mercury 198 isotope.

## II. Theory

The factors causing the physical limitation in the precision of setting of a photodetecting, optical interferometer can be classified generally as signal noise. The total noise impressed on the detected signal arises from individual effects of :

    (i) The statistical variation in the incident light quanta (photon noise).

    (ii) The shot noise in the photodetector tube.

    (iii) The thermal noise in the photodetector load resistor (Johnson noise).

    (iv) The randomness in amplification in the multiple stages of the photo-multiplier tube.

    (v) The flux variations in the light source.

The last of these has been examined (Hanes 1959 ; Smith 1960) and shown to be a slow variation which does not affect detection in a scanning interferometer where the scanning frequency is more than a few cycles per second. The first three cases, which are likely to be the more important, will be considered in detail. The effects of randomness of amplification have been examined by Bell (1960) and it has been shown that a decrease in the signal-to-noise ratio of the order of 30% can be expected.

### (a) Photon Noise

The following analysis is based on that presented by Hanes (1959). The sensitivity of setting is defined as the ratio of the order of interference $n$ to the smallest change in order $\delta n$ from the setting on a fringe peak which produces a difference signal equal to the root mean square (r.m.s.) value of the noise for that setting on the fringe peak. The r.m.s. noise level for a setting is given by

$$\left(\frac{\theta p \tau}{E} \int_{n_1}^{n_2} F(n) \mathrm{d}n\right)^{\frac{1}{2}}, \tag{1}$$

where $n_2$ is the order at the centre and $n_1$ the order at the edge of the interferometer " viewing " aperture and

    $\theta$ is the detector quantum efficiency (Rose 1946 ; Jones 1958),

    $p$ is the power available in each order of interference,

    $\tau$ is the time of observation on the fringe peak,

    $E$ is the energy of a photon, and is given by $hc\sigma$, where $\sigma$ is the wavenumber of the radiation and $h$ and $c$ have their usual meanings.

The source radiance for the 6056 Å line of krypton has been measured by Engelhard (1958) and it is possible to obtain the radiance of other lines and sources by comparison with this line. However, this gives the power $P$ at the lamp directly and not the power allowed to fall on the detector at a fringe peak. The signal at the detector is given by $P\mathscr{T}\mathscr{T}_0$, where $\mathscr{T}$ is the transmittance of the interferometer, and $\mathscr{T}_0$ is the transmittance of the rest of the optical system.

The power available is then given by

$$\frac{\pi^2 D^2}{4t\sigma} P\mathscr{T}\mathscr{T}_0, \tag{2}$$

where $D$ is the diameter of the interferometer plates,

    $t$ is the plate separation,

    $P$ is the source radiance,

and    $\mathscr{T}$ is equal to $T^2/(1-R)^2$ for the Fabry–Perot (where $T$ is the transmittance and $R$ the reflectance of each interferometer plate) and equal to $0\cdot5$ for the Michelson.

The intensity distribution of the Fabry–Perot interferometer, $F(n)$, is given by Krebs and Sauer (1953) as

$$F(n) = 1 + 2\sum_{k=1}^{\infty} G_k \cos 2\pi k n, \tag{3}$$

where

$$G_k = R^k \exp\left(-\pi^2 \mu^2 k^2/4 \ln 2\right),$$

and $\mu$ is the fraction of an order occupied by the spectral line width $w$ and equals $2tw$.

For a scanning interferometer, the order of interference changes sinusoidally and, with an amplitude of oscillation $a$, the intensity distribution becomes

$$F(n + a\cos\omega t) = 1 + 2\sum_{k=1}^{\infty} G_k \cos 2\pi k(n + a\cos\omega t).$$

This is the signal passed out of the photodetector to the other elements of the detecting circuit. If one of these elements is perfectly tuned to the oscillation frequency of the plates the signal allowed to pass through will be

$$-4\sum_{k=1}^{\infty} G_k \sin 2\pi nk\, 2J_1(2\pi ka)\cos\omega t,$$

where $J_1(2\pi ka)$ is the Bessel function of the first kind, of order one and of amplitude $(2\pi ka)$. The remaining portion of the detector output, together with the noise that lies out of the passband of the tuned element, is lost to the rest of the detecting circuit. If the oscillating signal is passed through a phase detecting device the final output for the instrumental signal is given by

$$F'(n) = -4\sum_{k=1}^{\infty} G_k J_1(2\pi ka)\sin 2\pi kn. \tag{4}$$

It is this form of the intensity distribution that should be used in the evaluation of equation (1).

The number of photons contributing to the final output for the instrumental signal is

$$\theta\frac{P\tau}{E}\int_{n_1}^{n_2} F'(n)\mathrm{d}n.$$

If the interferometer is oscillating about an integral order $n_0$, and if the radius of the " viewing " aperture in front of the photodetector is $2b$, the effective number of photons can be given as

$$2\theta\frac{P\tau}{E}\left|\int_{n_0}^{n_0+b} F'(n)\mathrm{d}n\right|,$$

which reduces to

$$4\theta\frac{P\tau}{E}\sum_{k=1}^{\infty}\frac{G_k}{\pi k}J_1(2\pi ka)(1-\cos 2\pi kb). \tag{5}$$

The r.m.s. noise level is thus given by

$$\left[4\theta\frac{P\tau}{E}\sum_{k=1}^{\infty}\frac{G_k}{\pi k}J_1(2\pi ka)(1-\cos 2\pi kb)\right]^{\frac{1}{2}}. \tag{6}$$

The difference signal is the output change from a setting at $n_0$ to a setting at $n_0+\delta n$, that is, the detected output is given by

$$\theta\frac{P\tau}{E}\left[\int_{n_0-b}^{n_0+b} F'(n)\mathrm{d}n - \int_{n_0-b+\delta n}^{n_0+b+\delta n} F'(n)\mathrm{d}n\right]. \tag{7}$$

But $\int_{n_0-b}^{n_0+b} F'(n)\mathrm{d}n = 0$ as $n_0$ is defined to be an integer and

$$\int_{n_0-b+\delta n}^{n_0+b+\delta n} F'(n)\mathrm{d}n = 4 \sum_{k=1}^{\infty} G_k J_1(2\pi ka) \int_{n_0-b+\delta n}^{n_0+b+\delta n} \sin 2\pi kn \mathrm{d}n.$$

The difference signal is thus

$$8\theta \frac{P\tau}{E} \delta n \sum_{k=1}^{\infty} G_k J_1(2\pi ka) \sin 2\pi kb. \tag{8}$$

Equating (6) and (8) and substituting for the difference of the integrals gives

$$\left(\frac{n}{\delta n}\right)_q = \left[\frac{\pi^2 D^2}{2hc}\tau\theta\frac{P}{w}\mathscr{T}_0 Q\right]^{\frac{1}{2}}, \tag{9}$$

where

$$Q = \mu\mathscr{T}16\frac{\{\sum_{k=1}^{\infty} G_k J_1(2\pi ka) \sin 2\pi kb\}^2}{\sum_{k=1}^{\infty} \frac{G_k}{\pi k} J_1(2\pi ka)(1 - \cos 2\pi kb)}. \tag{10}$$

Equation (9) agrees with Hanes' result but the form of the equivalent equation for $Q$ differs.

Figure 1 shows the magnitude of $Q$ as a function of $\mu$ for a series of reflectivities of dielectric, aluminium, and silver films. The dielectric films are assumed to have an absorption of 1%, and the values for the reflectance $R$,

TABLE 1

VALUES OF THE TRANSMITTANCES $\mathscr{T}$ USED FOR THE CALCULATION OF THE LIMITING PRECISION IN THE FABRY–PEROT INTERFEROMETER

| Reflectance $R$ | Transmittance $\mathscr{T}$ | | |
|:---:|:---:|:---:|:---:|
| | Dielectric | Silver | Aluminium |
| 0·94 | 0·694 | — | — |
| 0·83 | 0·886 | 0·585 | 0·222 |
| 0·73 | 0·927 | 0·605 | 0·396 |
| 0·61 | 0·949 | 0·318 | 0·444 |
| 0·42 | 0·966 | 0·297 | 0·459 |

and transmittance $\mathscr{T}$ of the aluminium and silver films are taken from the experimental results of Lennier, Lagarde, and Filippi (1959) and Trompette (1956) respectively. The transmittance values for the films are given in Table 1. Equation (10) shows that the sensitivity of setting varies with the size of aperture and the amplitude of oscillation. In the results presented in Figure 1 an amplitude of oscillation of one-eighth of an order has been assumed and the $Q$ factor for a range of aperture sizes calculated. The optimum value of $Q$ was then chosen from these results. A detailed examination of the effects of aperture size, and amplitude of oscillation will be given later.

Evaluation of the form of the factor $Q$ for the two-beam Michelson interferometer gives

$$Q = \mu \mathscr{T} 8\pi V J_1(2\pi a)(1 + \cos 2\pi b), \tag{11}$$
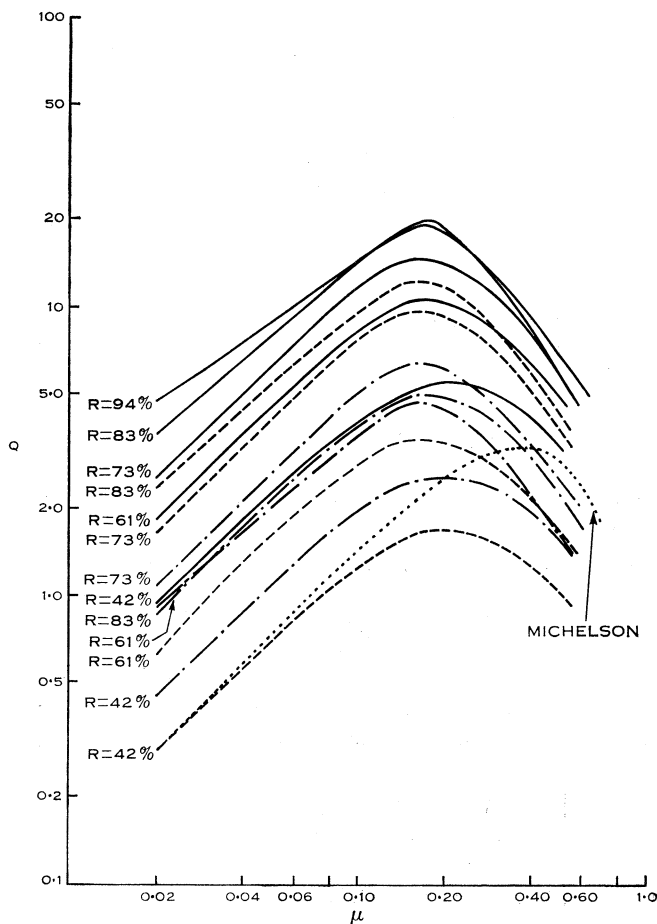
where

$$V = \exp(-\pi^2 \mu^2 / 4 \ln 2).$$



Fig. 1.—Quality of setting factor $Q$ (photon noise) as a function of the fraction of an order taken up by the spectral line width $\mu$. $a = 0 \cdot 125$, $b =$ optimum values.

Fabry–Perot :  dielectric films  ———
                silver films      – – –
                aluminium films   —·—
Michelson       ·····

From equation (11) the optimum value of $Q$ is obtained at a very small aperture size, and when the amplitude of oscillation $a$ is $0 \cdot 293$ of an order of interference. Under these conditions, the optimum value of $Q$ is obtained when $\mu$ is $0 \cdot 375$ and its value is $3 \cdot 33$.   The form of the variation of $Q$ with $\mu$ for the optimum values of $a$ and $b$ is given in Figure 1.

### (b) Shot Noise

Shot noise is the signal that occurs in an electron valve when the electrons are emitted at random times, and perform their transits without interaction. It occurs in vacuum photocells at reasonable light levels, and the r.m.s. noise level (current) is given by Bell (1960) as

$$(2ie\,d\nu)^{\frac{1}{2}},$$

where $e$ is the charge on a single electron, $d\nu$ the bandwidth of the circuit, and $i$ the mean current flowing in the valve.

For a scanning interferometer of the Fabry–Perot type, the number of photons contributing to the output of the photodetector in an observing time $\tau$ is $\theta(P\tau/E)I$, where $I$ is the total number of photons corresponding to the average steady current component of the intensity function $I_0$ and

$$I_0 = \int_{n_0-b}^{n_0+b} [1 + 2\sum_{k=1}^{\infty} G_k \cos 2\pi k(n + a\cos\omega t)]\mathrm{d}n.$$

Thus

$$I = 2b + 2\sum_{k=1}^{\infty} \frac{G_k}{\pi k} J_0(2\pi ka)\sin 2\pi kb,$$

where $J_0(2\pi ka)$ is the Bessel function of the first kind, of zero order and of amplitude $(2\pi ka)$.

The output current $i$ is given by

$$\theta \frac{pe}{E} I.$$

The bandwidth of the detecting circuit can be taken as $1/\tau$ without serious error and consequently the r.m.s. noise level in the current is given by

$$\left[ 2\theta \frac{pe^2}{E\tau} \left\{ 2b + 2\sum_{k=1}^{\infty} \frac{G_k}{\pi k} J_0(2\pi ka)\sin 2\pi kb \right\} \right]^{\frac{1}{2}}. \tag{12}$$

From equation (8) the current difference signal will be

$$8\theta \frac{pe}{E} \delta n \sum_{k=1}^{\infty} G_k J_1(2\pi ka)\sin 2\pi kb. \tag{13}$$

Equating (12) and (13) and remembering that $n = 2t\sigma$, and $\mu = 2tw$ we find

$$\left( \frac{n}{\delta n} \right)_s = \left[ \frac{\pi^2 D^2}{2hc} \tau\theta \frac{P}{w} \mathscr{T}_0 S \right]^{\frac{1}{2}}, \tag{14}$$

where

$$S = \mu \mathscr{T} 32 \frac{\{\sum_{k=1}^{\infty} G_k J_1(2\pi ka)\sin 2\pi kb\}^2}{2b + 2\sum_{k=1}^{\infty}(G_k/\pi k)J_0(2\pi ka)\sin 2\pi kb}. \tag{15}$$

Equation (14) is of the same form as the equivalent expression already obtained for the photon noise evaluation, equation (9). The function $S$ differs from $Q$, as would be expected from the nature of the noise source. For the Michelson interferometer it can be shown that

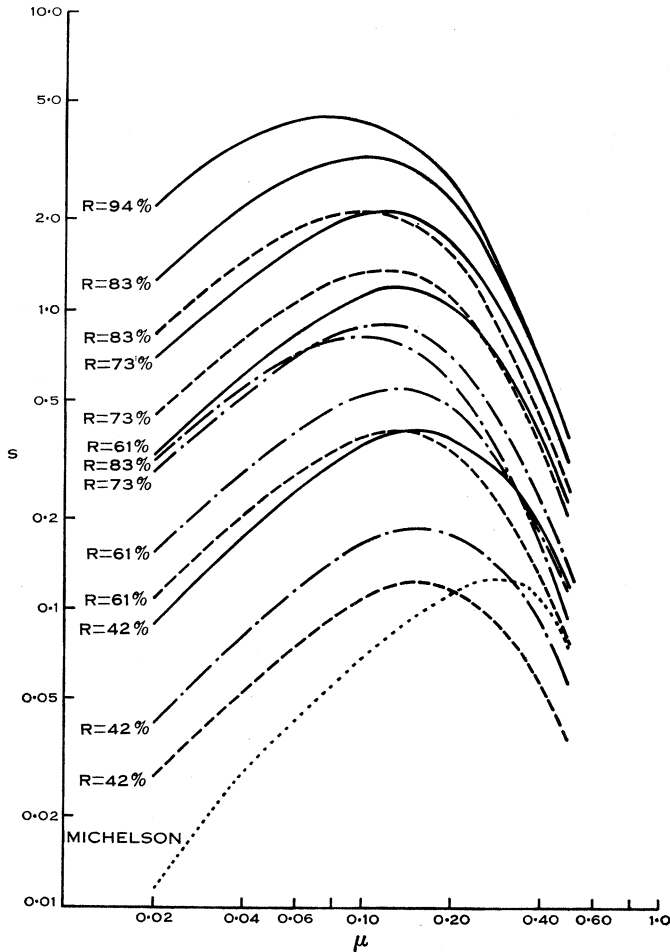$$S = \mu \mathscr{T} 8 \frac{\{VJ_1(2\pi a) \sin 2\pi b\}^2}{2b + (V/\pi)J_0(2\pi a) \sin 2\pi b}. \tag{16}$$



Fig. 2.—Quality of setting factor $S$ (shot noise) as a function of $\mu$. $a = 0 \cdot 125$, $b =$ optimum values.

|  |  |  |
|---|---|---|
| Fabry–Perot : | dielectric films | ——— |
|  | silver films | – – – |
|  | aluminium films | —·— |
| Michelson | - - - - - | |

The variation of the function $S$ with $\mu$ for the interferometers is given in Figure 2. The same series of Fabry–Perot coatings has been used, and the results, as before, have been calculated for the optimum aperture size. This was not the same value as for the quantum noise case.

### (c) Johnson Noise

Johnson noise is the signal induced in a resistor by the thermal movement of the electrons in the resistive material. This is of importance in the detection of small photocurrents as the effect occurs in the high value load resistor of the phototube. For this effect, the r.m.s. noise current is given by the relationship

$$I_{d\nu} = \left(4 \frac{kT}{R} d\nu\right)^{\frac{1}{2}}, \tag{17}$$

where, as before, $d\nu$ is the bandwidth of the circuit, and $I_{d\nu}$ is the r.m.s. signal in that bandwidth ; $R$ is the load resistance and $k$ and $T$ are the Boltzmann constant and the absolute temperature respectively.

From equation (13) the current difference signal at the load resistor will be

$$8 A \theta \frac{pe}{E} \delta n \sum_{k=1}^{\infty} G_k J_1(2\pi k a) \sin 2\pi k b, \tag{18}$$

where $A$ is the amplification in the multiple stages of the photomultiplier.

By equating (17) and (18) it follows that

$$\left(\frac{n}{\delta n}\right)_j = A \frac{\pi^2 D^2}{2hc} \theta e \tau^{\frac{1}{2}} \frac{P}{\sigma} \mathscr{T}_0 \sqrt{\left(\frac{R}{kT}\right)} J, \tag{19}$$

where

$$J = \mathscr{T} 4 \sum_{k=1}^{\infty} G_k J_1(2\pi k a) \sin 2\pi k b, \tag{20}$$

and the bandwidth is again taken as the reciprocal of the time constant of the detecting circuit. The expression for $J$ in the Michelson interferometer is

$$J = \mathscr{T} 2 V J_1(2\pi a) \sin 2\pi b. \tag{21}$$

### (d) Evaluation of Noise Factors

It has been shown that the limiting precision for the setting on a fringe, considering quantum and shot noise fluctuations, can be given by

$$(n/\delta n)_q = (\Delta Q)^{\frac{1}{2}}, \quad \text{and} \quad (n/\delta n)_s = (\Delta S)^{\frac{1}{2}},$$

where

$$\Delta = \frac{\pi^2 D^2}{2hc} \tau \theta \frac{P}{w} \mathscr{T}_0,$$

and the rest of the symbols have their previous meanings. In the evaluation of the interferometer constant $\Delta$ the m.k.s. system of units will be used, and an interferometer with a plate diameter of 1 in. will be considered. For convenience, the time constant of the detector circuit is taken as 1 sec ($d\nu = 1$ c/s). Engelhard (1958) has measured the power of the 6056 Å line of the krypton isotope lamp as $3 \cdot 0 \times 10^{-1}$. The quantum efficiency of the trialkali cell in this region of the spectrum is $7 \cdot 0 \times 10^{-2}$, and the half-width of the krypton radiation is $1 \cdot 4$ m$^{-1}$. For normal collimation and dispersion systems $\mathscr{T}_0$ can be about $0 \cdot 20$. Under these conditions

$$\Delta_{6056} = 4 \cdot 81 \times 10^{19}.$$

Thus, for a krypton source with an oscillating plate Fabry–Perot interferometer having silvered plates of 83% reflectance and an amplitude of scan of 0·125, the maximum precisions of setting for the quantum and shot effects are

$$(n/\delta n)_q = 2\cdot 42 \times 10^{10}, \quad \text{and} \quad (n/\delta n)_s = 1\cdot 78 \times 10^{10},$$

respectively.

For an evaluation of the maximum precision for the Johnson noise, the amplification in the photomultiplier tube may be taken to be in excess of $10^6$, and the load resistance to be half a megohm. For these values

$$(n/\delta n)_j = 7\cdot 08 \times 10^{13}.$$

It is obvious that, in comparison with the quantum and shot noise effects, the Johnson noise may be ignored as a limiting factor in the precision of setting in an optical interferometer.

### (e) Total Noise

The limiting precisions for three noise sources in a photodetecting optical interferometer have been calculated, and it has been shown that in practice only two of these need be considered. The quantity $\delta n$ has been defined as the change in order of interference necessary to give a signal change equal to the r.m.s. noise levels of each source in turn. Thus, at any one setting of the interferometer, the r.m.s. noise levels for the quantum and shot noise sources are given by

$$K(\delta n)_q, \quad \text{and} \quad K(\delta n)_s,$$

respectively, where $K$ is a constant, dependent only on the interferometer and its setting.

For discrete, non-interfering noise sources the total mean square noise is given by the sum of the mean square values of the individual components. Hence

$$K^2(\delta n)^2 = K^2\{(\delta n)_q^2 + (\delta n)_s^2\}, \tag{22}$$

and

$$(\delta n)_q^2 = n^2/\Delta Q, \quad \text{and} \quad (\delta n)_s^2 = n^2/\Delta S,$$

so that the total limiting precision, considering the quantum and shot effects, is

$$\left(\frac{n}{\delta n}\right)_t = \left(\frac{1}{\Delta Q} + \frac{1}{\Delta S}\right)^{-\frac{1}{2}} = \Delta^{\frac{1}{2}}\Phi, \tag{23}$$

where

$$\Phi = \left(\frac{QS}{Q+S}\right)^{\frac{1}{2}}. \tag{24}$$

But Bell (1960) has shown that the effect of randomness of amplification in the multiple stages of a photomultiplier tube is to give a decrease in the signal-to-noise ratio of 30%. The r.m.s. noise signal has already been obtained, and thus the limiting precision, taking into account the randomness of amplification, is given by

$$\left(\frac{n}{\delta n}\right) = \frac{\Delta^{\frac{1}{2}}}{1\cdot 3}\Phi. \tag{25}$$

The total noise function $\Phi$ has been evaluated for an amplitude of oscillation of one-eighth of a fringe spacing.   The form of the result is shown in Figure 3 for a series of Fabry–Perot interferometer coatings and for the Michelson interferometer.
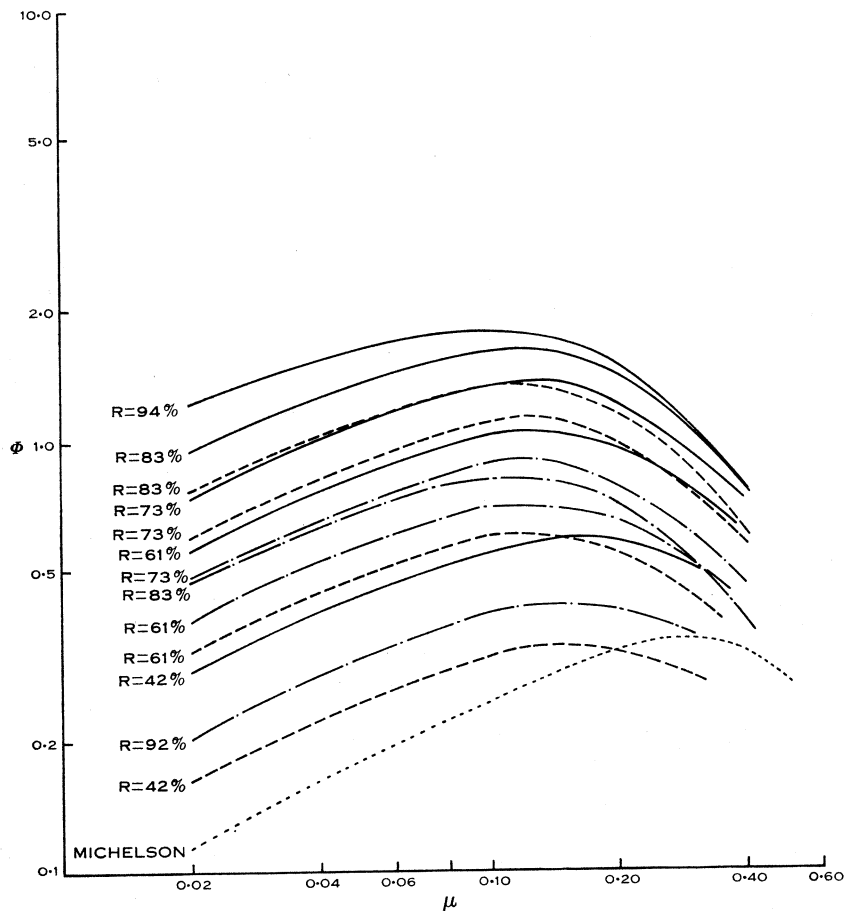


Fig. 3.—Total noise function $\Phi$ as a function of $\mu$.    $a = 0 \cdot 125$, $b =$ optimum values.

Fabry–Perot :   dielectric films    ———
                         silver films         – – –
                         aluminium films   —·—
Michelson  - - - - -

The results were calculated for a range of aperture sizes and the optimum values chosen.   The sizes of aperture to give maximum precision in the Fabry–Perot interferometer are shown in Figure 4 as a function of $\mu$ for a range of reflectivities.   The aperture size is independent of the transmittances of the reflecting films, and thus of the material of the film.   The effect of varying the amplitude of oscillation is examined in Figure 5.   It is clear that there is an optimum amplitude of oscillation for each value.   The relation between $\mu$ and $a$ is shown in Figure 6.
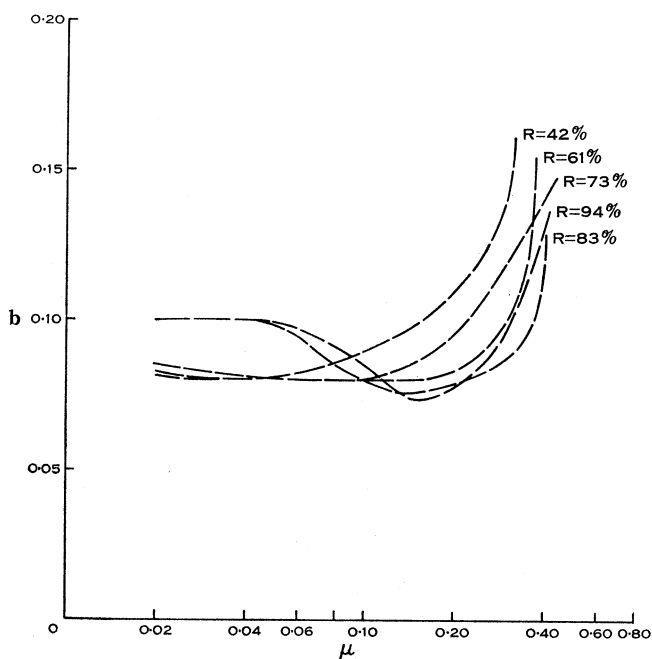
Fig. 4.—Optimum aperture dimension $b$ as a function of $\mu$.
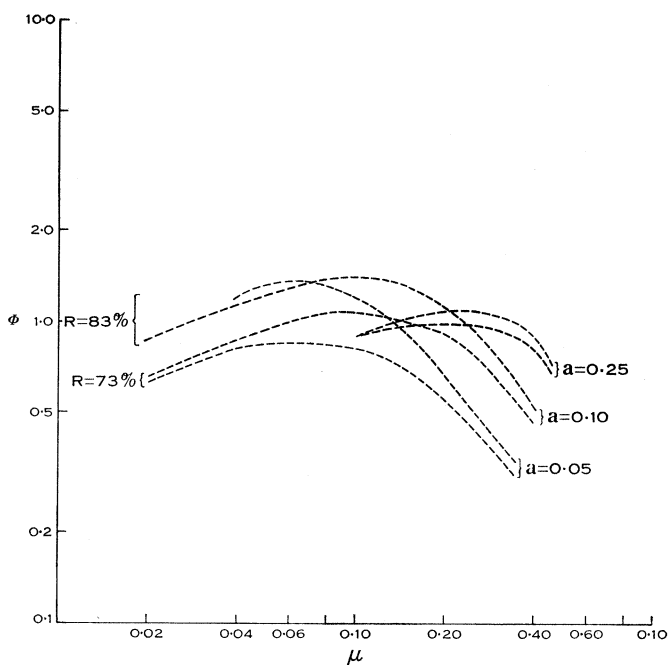Fabry–Perot ; $a = 0 \cdot 125$.



Fig. 5.—Variation of total noise function $\Phi$ with amplitude of
oscillation $a$ as a function of $\mu$.
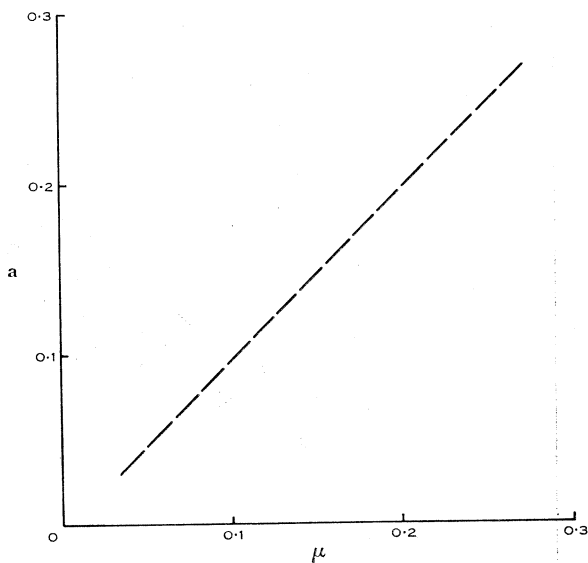Fabry–Perot ; silver films ; optimum apertures.

Fig. 6.—Optimum amplitudes of oscillation $a$ for maximum $\Phi$ as a function of $\mu$.
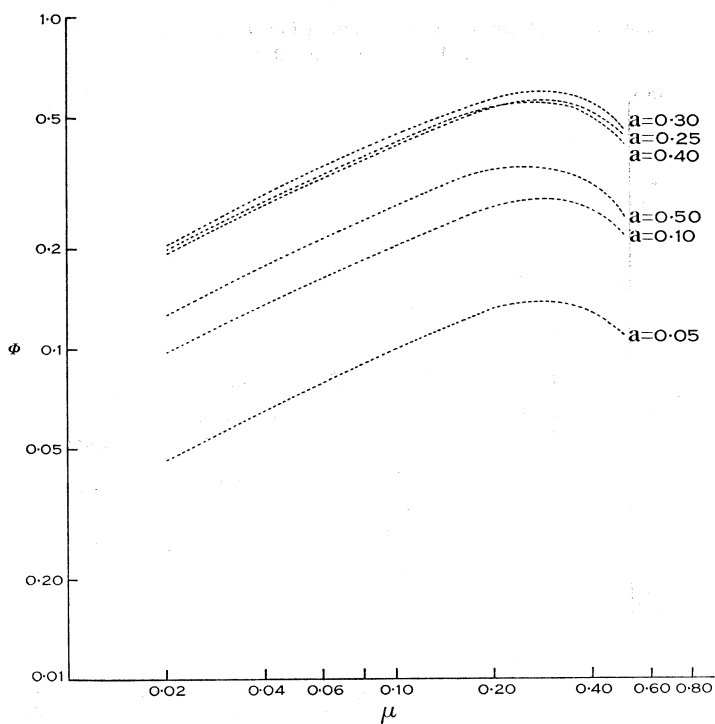
Fabry–Perot ;  silver films ;  optimum apertures.



Fig. 7.—Variation of total noise function $\Phi$ with amplitude of oscillation $a$ as a function of $\mu$.

Michelson ;  $b = 0.20$.

In the Michelson interferometer, the optimum aperture size was found to be independent of the plate separation and of magnitude 0·20 orders. The effect of varying the amplitude of oscillation in the oscillating-plate Michelson interferometer is shown in Figure 7. The maximum value of the total noise function $\Phi$ is 0·605 at an amplitude of oscillation of about 0·32.

### III. EXPERIMENTAL

The oscillating-plate interferometer used in the examination of the limiting sensitivity has been described in detail elsewhere (Bruce and Hill 1961). A diagram of the interferometer is given in Figure 8. It consists of two plate holders mounted in an invar trough. Electromagnetic controls allow one of the plates to be tilted about two mutually perpendicular axes, while the other can be moved, with a parallel motion, over three or four orders of interference. The
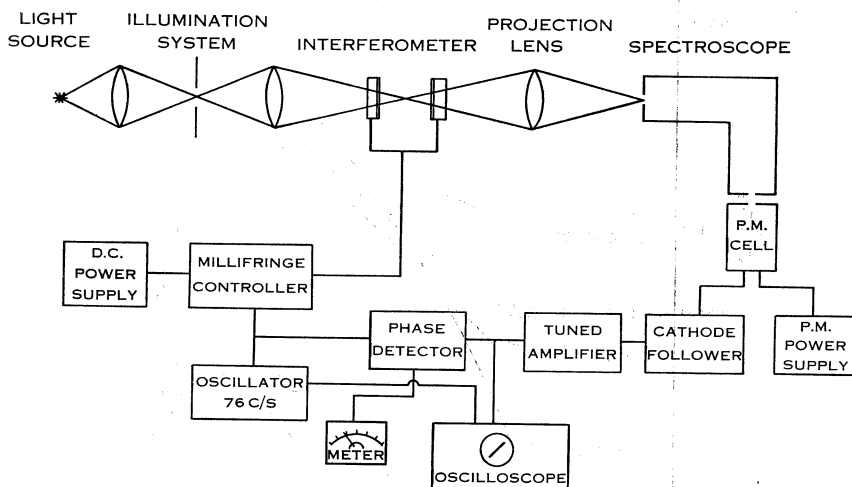


Fig. 8.—Block diagram of Fabry–Perot interferometer and photodetection system.

displacement of this plate is directly proportional to the current passing through the driving coil. A decade current controller has been designed to give, accurately, current increments of one-thousandth of the current required to displace the plate through one complete order. As the control mechanism is completely electrical, measurements can be carried out in vacuum, thereby eliminating one of the sources of error of the air pressure controlled interferometers. The driving coils have been designed to give a very small temperature drift in the instrument.

A lens of focal length 210 mm was used to project the haidinger ring pattern on to the slit of a spectrograph. The light from the centre of the pattern was passed through an aperture 0·4 mm in diameter and allowed to fall on the cathode of a trialkali photomultiplier cell. The signal from the interferometer was modulated at a frequency of 76 c/s by superimposing an a.c. signal on the driving current through the translation plate holder. The amplitude of the signal was such that the fringes were oscillated through a double amplitude of about a quarter of an order.

The signal from the photodetector was passed to a battery-operated cathode follower unit and then to a tuned amplifier. The signal from the tuned amplifier was displayed on the $Y$ plates of an oscilloscope, the $X$ signal being the driving current through the plate coil. The oscilloscope acts as a first-stage detector, being sensitive enough to show settings on a fringe peak to within $\pm 0\cdot001$ of a fringe spacing.

The voltage from the tuned amplifier was also used as the input of a phase-detecting circuit. A meter indication gave the zero phase condition when a setting was made on the peak of a fringe. Calibration of the meter showed that,
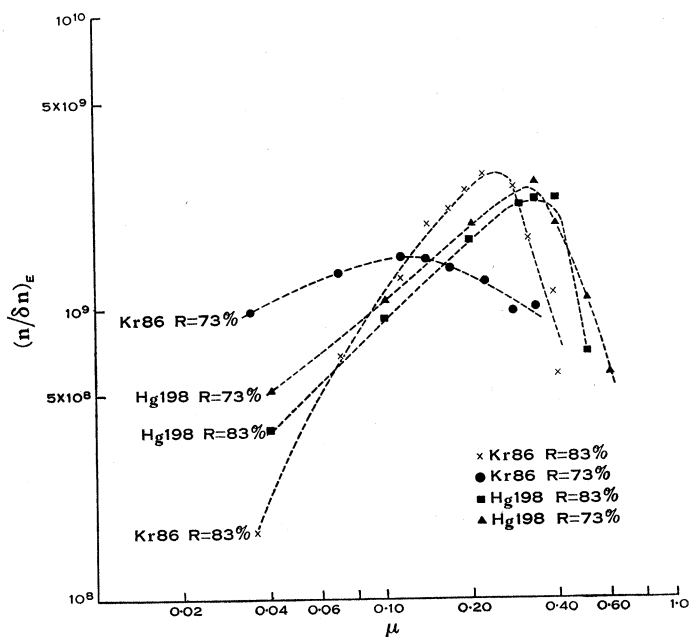


Fig. 9.—Precision of setting (experimental), $(n/\delta n)_E$ for Kr 86 6056 Å and Hg 198 5461 Å.

Fabry–Perot; silver films; $b$ as in Table 2.

over a range of $\pm 0\cdot005$ fringes, the meter current was directly proportional to the fringe displacement from the setting on a peak. This allowed a series of readings to be made as the interferometer spacing drifted, owing to thermal effects, over a range of about one-hundredth of a fringe spacing. Meter and dial readings were taken for settings on two adjacent fringe peaks at equal time intervals. From these readings the sensitivity of setting on a single fringe was calculated to $0\cdot01$ millifringe.

It should be stated that, when the measurements were being made, the interferometer was used under vacuum conditions in a massive chamber of high thermal capacity, and in a room the temperature of which was closely controlled. As the fringe drift under these conditions was only a few thousandths of a fringe in 15 min, a thermostatically controlled water jacket was considered unnecessary.

The setting procedure of fringe A–fringe B–fringe A, and so on, at accurate time intervals of 10 sec between each setting, eliminated any significant errors from fringe drift, where setting sensitivities were of the order of $0 \cdot 0001$ fringe. It was considered that this procedure was preferable to trying to use a thermostatically controlled chamber to stop fringe drifts of the order of $0 \cdot 0001$ fringe.

Measurements were made for two plate reflectivities of silver films, and for two spectral lines, the 6056 Å line of krypton 86 isotope and the 5461 Å line of mercury 198 isotope. The krypton light source was an Engelhard-type lamp immersed in liquid air at 63 °K and operated at a current density of $0 \cdot 3$ A/cm²; the mercury source was a Meggers-type high frequency discharge lamp cooled to 11 °C. The results obtained are shown as a function of $\mu$ in Figure 9.

The photoelectric Fabry–Perot interferometer can be used with either parallel or non-parallel light passing through the interferometer. If the incident light is parallel, an image of the source aperture is formed in the plane of the aperture in front of the photocell. This should give maximum illumination of the instrument, but with the capillary source of the krypton discharge it can give rise to an unevenness in the field which would affect the setting point of the interferometer. It was found that it was better to use non-parallel incident light and obtain a well-illuminated, even field in the plane of the aperture. The transmittance of the optical components of the interferometer was measured under these conditions, and also in parallel light. The values obtained were

Collimated light $\mathscr{T}_0 = 0 \cdot 14$
Non-collimated light $\mathscr{T}_0 = 0 \cdot 15$.

The characteristics of the silver coatings of the plates were

| Radiation (Å) | Kr 6056 | | Hg 5461 | |
|---|---|---|---|---|
| Reflectance $R(\%)$ | 83 | 73 | 83 | 73 |
| Transmittance $\mathscr{T}$ | $0 \cdot 293$ | $0 \cdot 289$ | $0 \cdot 222$ | $0 \cdot 232$ |

The effective powers of the 5461 Å line of a mercury 198 electrodeless lamp and of the 6438 Å line of a cadmium 114 electrodeless lamp (Bruce and Hill 1961) were measured by comparison with the krypton 6056 Å line from the standard krypton lamp. The power of the latter radiation was measured accurately by Engelhard (1958). The results express the function $\theta P$, where $P$ is the power of the radiation and $\theta$ the detector quantum efficiency of the trialkali cell at these particular wavelengths. The results were $1 \cdot 38$ m.k.s. units for the mercury radiation at a power input of 50 W, and for the cadmium $0 \cdot 442$ m.k.s. units at a power input of 70 W. Thus, for the theoretical interferometer considered earlier, for which the interferometer constant $\Delta_{6056}$ was $4 \cdot 81 \times 10^{19}$, the corresponding values of the constant are $\Delta_{5461} = 1 \cdot 47 \times 10^{20}$ and $\Delta_{6438} = 3 \cdot 39 \times 10^{19}$ respectively.

## IV. Discussion

The discussion on the determination of the limiting precision is given in four parts. First, a comparison is made between the experimental and the theoretical limiting precisions for a silver reflecting film Fabry–Perot interferometer; then the optimum conditions for the best use of a Fabry–Perot are

F

considered.   This examination is then repeated for the Michelson interferometer, and a comparison is made between the precisions of setting attainable in the two instruments.   It is assumed that spectral line profiles are symmetrical in this discussion.

### (a) Comparison of Experimental and Theoretical Sensitivity of Setting

In the determination of the maximum precision of setting of the oscillating-plate Fabry–Perot interferometer, the amplitude of scan was chosen to be approximately one-eighth of an order of interference.   This was set by visual examination of the oscillating fringe pattern in the plane of the plate of the spectrograph.

TABLE 2

EXPERIMENTAL APERTURE SIZES FOR THE RANGE OF $\mu$ INVESTIGATED

| Line Width $\mu$ | Aperture Dimension $b$ | | Line Width $\mu$ | Aperture Dimension $b$ | |
|---|---|---|---|---|---|
| | Kr Radiation | Hg Radiation | | Kr Radiation | Hg Radiation |
| 0·02 | 0·006 | 0·0054 | 0·30 | 0·089 | 0·080 |
| 0·06 | 0·018 | 0·016 | 0·40 | 0·118 | 0·107 |
| 0·10 | 0·030 | 0·027 | 0·50 | 0·147 | 0·133 |
| 0·20 | 0·060 | 0·054 | | | |

The theoretical limiting precision curve calculated for $a = 0·125$, and for the experimental aperture sizes listed in Table 2 showed that peak precisions occurred at a value of $\mu = 0·125$, which was in good agreement with the curve computed for optimum values of aperture sizes (Fig. 3).   This showed that aperture size has a relatively small effect on the form of the curves.

TABLE 3

AMPLITUDES OF SCAN FOR FIGURE 10

| Radiation (Å) | Reflectivity $R$ (%) | Amplitude $a_e$ | Radiation (Å) | Reflectivity $R$ (%) | Amplitude $a_e$ |
|---|---|---|---|---|---|
| 6056 | 83 | 0·20 | 5461 | 83 | 0·25 |
| | 73 | 0·07 | | 73 | 0·25 |

The $\mu$ values for peak precision obtained experimentally however with $a \approx 0·125$ were rather different as shown in Figure 9.   As these $\mu$ values are affected significantly by the amplitude of scan (Fig. 6), the theoretical precision curves were then computed for amplitudes of scan $a_e$ which brought the $\mu$ values for peak precision into good agreement with those already obtained experimentally.   The values of $a_e$ are given in Table 3, and it is reasonable to assume that these were the actual experimental values.   The computed curves for amplitudes of scan $a_e$ and the particular interferometer constants of transmittance, reflectance, aperture size, and time constant are given in Figure 10.

It is apparent from Figure 9, which shows the experimentally determined curves, and Figure 10, which shows the equivalent theoretical curves, that the forms of the change in precision with increasing plate separation are similar. The region of the curves, for the larger amplitudes of oscillations, are less peaked in the theoretical cases than in the experimental, and the experimental peak values are, on the average, less than the theoretical in the ratio $1 : 1 \cdot 8$.
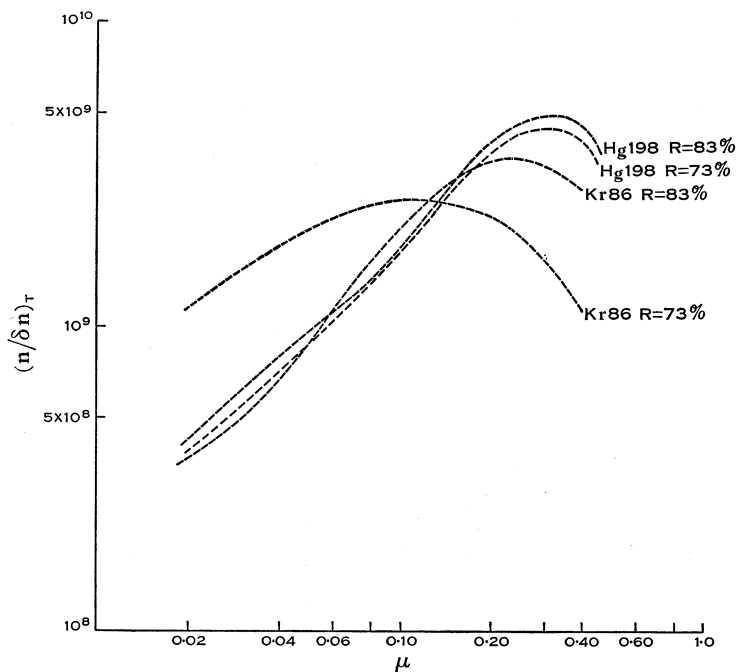


Fig. 10.—Precision of setting (theoretical), $(n/\delta n)_T$ for Kr 86 6056 Å and Hg 198 5461 Å.

Fabry–Perot ; silver films, $a_e$ as in Table 3 ; $b$ as in Table 2.

The differences between the experimental and theoretical precisions of setting can be due to a variety of causes. If the interferometer had been mis-aligned, then the transmittance of the system would be less than the measured value of $\mathscr{T}_0$ which was obtained some time later. This is not a likely source of error as the measurements were made over a period of time and, during this period, the alignment of the interferometer was frequently checked.

The more likely causes are either a source of signal noise in the detecting circuit or in the interferometer itself, or slight imperfections in the interferometer plates. Noise could arise in the interferometer through the effects of floor vibration acting on the elastic membranes carrying the optical flats. This effect was not noticeable, as the interferometer was mounted on a very efficient antivibration mounting. The sources of noise in the signal would cause a decrease in the signal-to-noise ratio in the same way as the random amplification in the photomultiplier stages.

Signal noise would affect the magnitude of the limiting precision, but cannot be used to explain the sharper cut-off in the precision as a function of $\mu$-curves at the higher values of $\mu$. Consideration of surface errors in the plates suggests that both these effects can be explained. Plate roughness in the interferometer will scatter the incident light and increase the effective line width. The latter will become more prominent at small values of plate separation, where there are many multiple reflections, and will shift the effective value of the halfwidths towards longer plate separations. This will have two effects. First, the scattering will cause a loss in light transmission, and hence a decrease in the limiting precision, and then the plate separation effect will cause the experimental values of $\mu$ to be found at larger than the theoretical values for small $\mu$, and will introduce some asymmetry into the curves. As the effects are less important for large values of $\mu$, the curves will be formed with a sharper peak and a much more rapid fall of precision past the peak value.

The agreement between the forms of the limiting precision of setting curves is such that the theory may be accepted as giving a reasonably reliable guide to the limiting precision of setting on a fringe peak in an optical interferometer, and giving a good estimate of the changes in precision that can be expected for variations in the experimental conditions of use of the instruments.

One point of particular interest is that the comparison between the experimental and theoretical results is better for the krypton light source than the mercury. The only experimental difference in the determination of these results is that of the light sources. This could mean that the discharge process in the high frequency mercury lamp gives a more random energy output than the direct current discharge in the krypton lamp or that the radio frequency power supply of the mercury lamp was causing a noise signal in the detector circuit.

### (b) *Examination of Optimum Conditions for the Fabry–Perot Interferometer*

It has already been shown in graphical form (Figs. 3 and 5) how the optimum precision of setting on a peak of a fringe varies with the amplitude of oscillation, the reflectivity of the plates, and the interferometer spacing. From the graphs, and the evaluation of the interferometer constant $\Delta$, some general conclusions on the optimum conditions can be formed.

(i) *Transmittance of the Instrument.*—Two transmittance values have been considered, that of the interferometer, and that of the rest of the instrument. Maximum sensitivity can be achieved by proper design and blooming of the optical elements of the collimation system, interferometer, and dispersion system. The transmittance of the interferometer can be increased by the use of highly reflecting dielectric multilayers, but as the reflectivity of these becomes high, the loss of light due to the small absorption and scattering effects becomes significant, and the transmittance is decreased. Little increase in sensitivity is obtained for reflectivities higher than 90%. Unfortunately, these coatings have a high wavelength dispersion which makes them unsuitable for wavelength comparisons.

(ii) *Amplitude of Oscillation.*—The particular advantage of the oscillating Fabry–Perot interferometer is that the amplitude of oscillation may be chosen

to give optimum precision for every spacing of the interferometer plates (Fig. 6). In this way it is possible to keep the precision within 10% of the maximum value over the spectral range $\mu = 0 \cdot 025 - 0 \cdot 25$ ($t = 10 - 100$ mm for 6056 Å).

The optimum amplitude of oscillation is about $0 \cdot 10$ of a fringe spacing (Fig. 5). This gives the maximum precision at a value of $\mu$ of $0 \cdot 10$.

For the case of the silver-coated interferometer ($R = 83\%$, $\mathscr{T} = 0 \cdot 585$), and the 6056 Å line of krypton 86, the maximum precision at $\mu = 0 \cdot 10$ is $7 \cdot 46 \times 10^9$. This means that the fringe fraction to be measured is about $1 \cdot 6 \times 10^{-5}$ of a fringe. This sensitivity would be extremely difficult to achieve in practice.
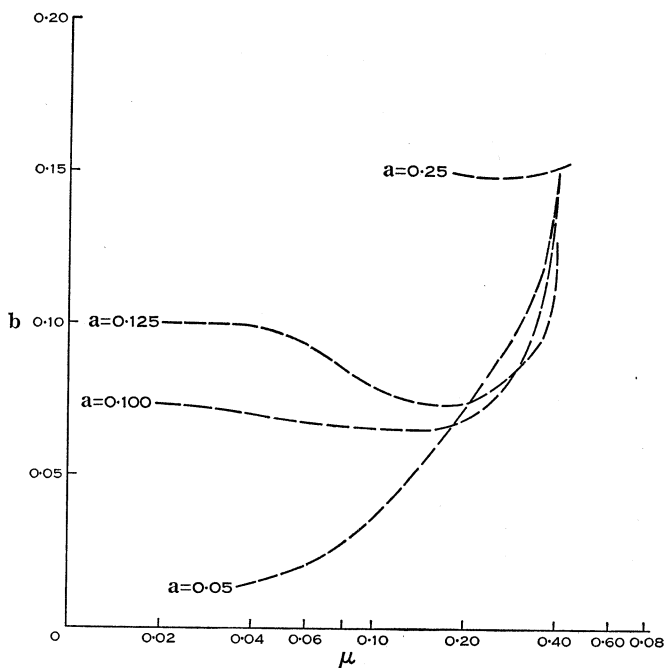


Fig. 11.—Optimum aperture dimension $b$ as a function of $\mu$, and $a$.
Fabry–Perot ; $R = 83\%$.

If, however, $\mu$ is allowed to be $0 \cdot 25$, then the maximum precision drops by only 10% and the corresponding fringe fraction to be measured is $4 \times 10^{-5}$, which is more practicable.

An even higher sensitivity is required in the detection system when the more powerful mercury green line is examined with dielectric plates in the interferometer. With a reflection coefficient of 94% and an amplitude of scan of $0 \cdot 10$, a precision of $1 \cdot 96 \times 10^{10}$ can be achieved, and the corresponding fringe fraction in this case is $4 \cdot 6 \times 10^{-6}$ of a fringe.

(iii) *Interferometer " Viewing " Aperture.*—The optimum aperture for an amplitude of scan of $0 \cdot 125$ has been given in Figure 4 for the range of reflectivities examined. It is also a function of the amplitude of scan as is shown in Figure 11. In these diagrams is shown the optimum " viewing " aperture $b_0$ for the reflectivity

83%. The aperture effect is not great. Figure 12 shows the total noise factor as a function of the aperture size $b$ for a range of values of $\mu$.

(iv) *Choice of Interferometer Constants.*—The limiting precision can be increased by altering the factors which determine the interferometer constant $\Delta$, that is, an increase can be obtained by increasing the period of the detector time constant. The value used in the experimental work was $1 \cdot 2$ sec and this has been found to be suitable. If the detector time constant is made too long, measurements have to be taken over a correspondingly longer period. This gives rise to observer fatigue, and causes an increased error due to thermal creep in the interferometer. The most important constant is $D$, the diameter of the interferometer plates. The nature of the effect of out-of-flatness of the plates has not been considered in detail, apart from a suggestion that it would
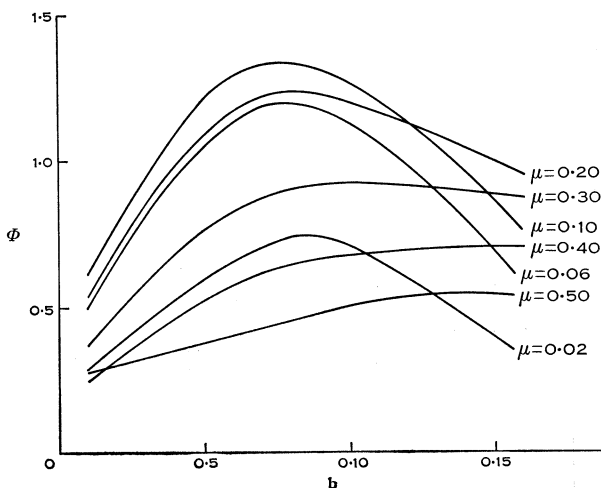


Fig. 12.—Variation of total noise function $\Phi$ as a function of the aperture dimension $b$ for a range of $\mu$ values. Fabry–Perot; $a = 0 \cdot 125$; $R = 83\%$.

give rise to a decrease in the limiting precision, and a sharper cut-off in the precision/plate separation curves. For this reason the aperture in the interferometer was limited to 1 in. diameter. This portion of the 2 in. diameter plates was flat to within 1/50 of a wavelength. Some increase in sensitivity may be obtained by using the full 2 in. surface, but it is not considered that the precision would be doubled.

The trialkali cathode photomultiplier cell is the most efficient detector of optical radiation at the present time. Cooling of the tube has been suggested as a means of decreasing the dark current value; as this would only affect the Johnson noise, which has been shown to be negligible, it would not seem to be necessary.

(c) *Examination of Optimum Conditions for the Michelson Interferometer*

The Michelson interferometer gives an easier assessment of the optimum working conditions. The transmittance of the instrument cannot be varied and for the optimum performance the order of aperture size must be $0 \cdot 20$ for

all plate separations. The optimum amplitude of scan is not very critical. The actual value is $0 \cdot 325$ but if the amplitude is within the range $0 \cdot 225$–$0 \cdot 415$, better than $90\%$ of the optimum value of $\Phi$ will be obtained. This can be seen from Figure 13, in which the maximum values of $\Phi$ for each amplitude of scan (Fig. 7) are plotted as a function of the amplitude.

From Figure 13 it can also be seen that the maximum value of $\Phi$ is $0 \cdot 61$. The plotted values all occur about the value of $\mu$ of $0 \cdot 30$. There is a little shift for large $a$ to smaller $\mu$ values but this is very slight and in practice could be disregarded.
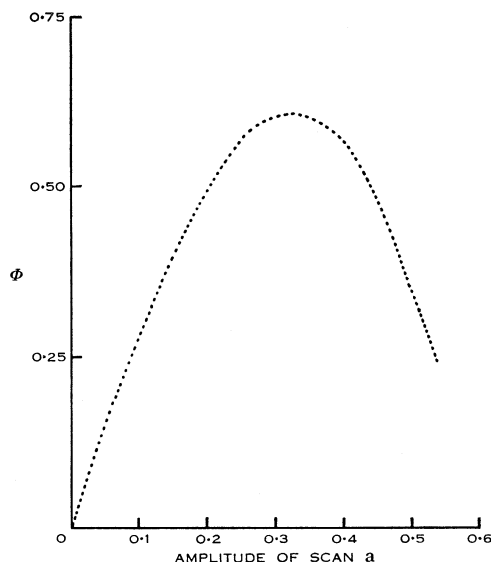


Fig. 13.—Variation of the total noise function $\Phi$
as a function of the amplitude of oscillation $a$.
Michelson ; $\mu = 0 \cdot 3$.

### (d) Precision of Setting n/δn and Wavelength Measurement

Some optimum conditions of use for the oscillating-plate interferometer and the highest or optimum precision of setting on a fringe peak $(n/\delta n)_0$ are given in Table 4. The interferometer constants are those calculated earlier for the interferometer of plate diameter 1 in., detector time constant 1 sec, a trialkali photomultiplier cell, and a transmittance $\mathscr{T}_0$ of $0 \cdot 20$.

In the determination of small wavelength shifts, pointings have to be carried out on two fringe patterns. The fringe spacing on one pattern has to be measured, requiring two pointings, and the fringe shift between the standard and the varying pattern has to be measured, requiring two further pointings. From signal noise theory, as the two intensity distributions are incoherent, the total signal change equal to the mean square noise level will be given by the sum of the signal changes equal to each of the mean square noise levels for the four pointings. If the r.m.s. noise signal for each pointing is $\delta n$ then the expression for the total noise signal can be written in the form

$$K^2(\delta n)_{\delta\lambda}^2 = K^2 4(\delta n)^2,$$

R. M. HILL AND C. F. BRUCE

TABLE 4

MAXIMUM PRECISION OF SETTING

| Interferometer | Spectral Line (Å) | $\Delta\sigma$ (m$^{-1}$) | Coating | Reflectance $R$ | Transmittance $\mathscr{T}$ | Plate Separation $t_0$ (mm) | Scan Amplitude $a_0$ (orders) | Aperture $b_0$ (orders) | Total Noise Function $\Phi$ | Precision $(n/\delta n)_0$ |
|---|---|---|---|---|---|---|---|---|---|---|
| Fabry–Perot .. | Kr 86 6056 | 1·4 | Dielectric | 94% | 0·694 | 35·7 | 0·10 | 0·07 | 2·10 | $1·12 \times 10^{10}$ |
| | Hg 198 5461 | 2·1 | ,, | ,, | ,, | 23·8 | ,, | ,, | 2·10 | $1·96 \times 10^{10}$ |
| | Cd 114 6438 | 2·9 | ,, | ,, | ,, | 17·3 | ,, | ,, | 2·10 | $9·39 \times 10^{9}$ |
| | Kr 86 6056 | 1·4 | Silver | 83% | 0·585 | 35·7 | 0·10 | 0·07 | 1·40 | $7·46 \times 10^{9}$ |
| | Hg 198 5461 | 2·1 | ,, | ,, | ,, | 23·8 | ,, | ,, | 1·40 | $1·31 \times 10^{10}$ |
| | Cd 114 6438 | 2·9 | ,, | ,, | ,, | 17·3 | ,, | ,, | 1·40 | $6·26 \times 10^{9}$ |
| | Kr 86 6056 | 1·4 | Aluminium | 73% | 0·396 | 35·7 | 0·10 | 0·07 | 0·87 | $4·64 \times 10^{9}$ |
| | Hg 198 5461 | 2·1 | ,, | ,, | ,, | 23·8 | ,, | ,, | 0·87 | $8·14 \times 10^{9}$ |
| | Cd 114 6438 | 2·9 | ,, | ,, | ,, | 17·3 | ,, | ,, | 0·87 | $3·89 \times 10^{9}$ |
| Michelson .. | Kr 86 6056 | 1·4 | | | | 107 | 0·325 | 0·20 | 0·605 | $3·22 \times 10^{9}$ |
| | Hg 198 5461 | 2·1 | | | | 71·4 | 0·325 | 0·20 | 0·605 | $5·64 \times 10^{9}$ |
| | Cd 114 6438 | 2·9 | | | | 51·7 | 0·325 | 0·20 | 0·605 | $2·70 \times 10^{9}$ |

$\Delta_{6056} = 4·81 \times 10^{19}$ ; $\Delta_{5461} = 1·47 \times 10^{20}$ ; $\Delta_{6438} = 3·39 \times 10^{19}$

where $(\delta n)_{\delta\lambda}$ is the r.m.s. noise level for the measurement of the wavelength shift $\delta\lambda$.

But it has already been shown that

$$\left(\frac{n}{\delta n}\right) = \frac{\Delta^{\frac{1}{2}}}{1\cdot3}\Phi,$$

and hence

$$\left(\frac{n}{\delta n}\right)_{\delta\lambda} = \frac{\Delta^{\frac{1}{2}}}{2\cdot6}\Phi = \tfrac{1}{2}\left(\frac{n}{\delta n}\right)_0,$$

where the symbols have their previous meanings.

Thus, for example, the best possible precision to be expected for Doppler and Stark shifts in the 6056 Å line of krypton 86 is about $6\times10^9$ (see Table 4).

The fundamental equation for the measurement of the wavelength $\lambda_B$ in terms of the wavelength of a known radiation $\lambda_A$ is

$$\lambda_B = \lambda_A\frac{n_{A2}-n_{A1}}{n_{B2}-n_{B1}} = \lambda_A\frac{N_A}{N_B} = \lambda_A R, \tag{26}$$

where $n_{A2}$ is the order of interference for $\lambda_A$ at a large path difference,

$n_{A1}$ is the order of interference for $\lambda_A$ at a small path difference.

$n_{B2}$ is the order of interference for $\lambda_B$ at a large path difference,

$n_{B1}$ is the order of interference for $\lambda_B$ at a small path difference.

In the determination of $n_{A2}$ and $n_{A1}$ three pointings for each are required, two for the fringe spacing and one for the actual measurement, but only one pointing is required to determine $n_{B2}$ and $n_{B1}$. By suitable adjustment of the amplitude of scan it can be assumed that the total noise factor for all these pointings is the same. By application of the statistical theory of errors it can be shown that the error in obtaining $n_{A2}$ and $n_{A1}$ is $\sqrt{3}(\delta n)_A$ for each, and that the error in obtaining either $n_{B2}$ or $n_{B1}$ is $(\delta n)_B$.

It follows directly that the error in $n_{A2}-n_{A1}$ is $\sqrt{6}(\delta n)_A$ and in $n_{B2}-n_{B1}$ is $\sqrt{2}(\delta n)_B$ which we let equal $E_A$ and $E_B$ respectively.

If the r.m.s. noise signal obtained in determining $R$ is $\delta R$, then it is given by

$$\frac{N_A}{N_B}\left\{\left(\frac{E_A}{N_A}\right)^2+\left(\frac{E_B}{N_B}\right)^2\right\}^{\frac{1}{2}},$$

but we may take $N_A\approx n_A = n_{A2}$ since $n_{A2}\gg n_{A1}$

and $N_B\approx n_B = n_{B2}$ since $n_{B2}\gg n_{B1}$

hence

$$\delta R = R\left\{6\left(\frac{\delta n}{n}\right)_A^2+2\left(\frac{\delta n}{n}\right)_B^2\right\}^{\frac{1}{2}}.$$

But it has already been shown that

$$\left(\frac{\delta n}{n}\right)_A^2 = \frac{(1\cdot3)^2}{\Delta_A\Phi_A^2}, \text{ and } \left(\frac{\delta n}{n}\right)_B^2 = \frac{(1\cdot3)^2}{\Delta_B\Phi_B^2},$$

so that

$$\frac{R}{\delta R} = \left\{\frac{10\cdot14}{\Delta_A\Phi_A^2}+\frac{3\cdot38}{\Delta_B\Phi_B^2}\right\}^{-\frac{1}{2}}$$

where $R/\delta R$ is the precision of wavelength determination.

R. M. HILL AND C. F. BRUCE

TABLE 5

MAXIMUM PRECISION OF WAVELENGTH COMPARISON

| Interferometer | Spectral Lines | | Coating | Reflect- ance $R$ | Plate Separation $t$ (mm) | Scan Amplitude $a$ (orders) | Aperture $b$ (orders) | Total Noise Function | | Precision $R/\delta R$ |
| --- | --- | --- | --- | --- | --- | --- | --- | --- | --- | --- |
| | A | B | | | | | | $\Phi_A$ | $\Phi_B$ | |
| Fabry–Perot | Kr 86 6056 | Hg 198 5461 | Dielectric | 94% | 28·5 | 0·10 | 0·066 | 1·86 | 1·86 | $3\cdot85\times10^9$ |
| | | | Silver | 83% | 28·5 | 0·10 | 0·066 | 1·40 | 1·40 | $2\cdot90\times10^9$ |
| | | | Aluminium | 73% | 28·5 | 0·10 | 0·066 | 0·95 | 0·95 | $1\cdot97\times10^9$ |
| | Kr 86 6056 | Cd 114 6438 | Dielectric | 94% | 25·0 | 0·10 | 0·066 | 1·82 | 1·82 | $3\cdot06\times10^9$ |
| | | | Silver | 83% | 25·0 | 0·10 | 0·066 | 1·38 | 1·38 | $2\cdot32\times10^9$ |
| | | | Aluminium | 73% | 25·0 | 0·10 | 0·066 | 0·93 | 0·93 | $1\cdot56\times10^9$ |
| Michelson  .. | Kr 86 6056 | Hg 198 5461 | | | 78·6 | 0·32 | 0·20 | 0·59 | 0·59 | $1\cdot22\times10^9$ |
| | Kr 86 6056 | Cd 114 6438 | | | 65·5 | 0·32 | 0·20 | 0·57 | 0·57 | $0\cdot96\times10^9$ |

$\Delta_{6056} = 4\cdot81 \times 10^{19}$ ;   $\Delta_{5461} = 1\cdot47 \times 10^{20}$ ;   $\Delta_{6438} = 3\cdot39 \times 10^{19}$

The precision of wavelength comparison has been calculated for the 5461 Å line of mercury 198 and the 6438 Å line of cadmium 114, each compared against the 6056 Å line of krypton 86.    The results are given in Table 5.

## V. Conclusions

The limiting precision in a scanning optical interferometer has been examined, and it has been found that the photon noise, shot noise, and randomness of amplification in the photomultiplier tube are important, but that the Johnson noise in the load resistor of the phototube can be neglected.    Of the photon and shot noises, the latter is the more prominent in the evaluation of the total noise factor.

The limiting precision has been expressed as the product of two quantities, the total noise factor $\Phi$ and the instrumental factor $\Delta$.    The former is only dependent on the type of interferometer, and the evaluation given is complete for the Fabry–Perot and Michelson instruments.    The instrumental factor is a function of the particular instrument constants.

The optimum precision of setting in a scanning interferometer can reach a higher limit with the Fabry–Perot interferometer than with the Michelson interferometer.    With silver films of high quality, the Fabry–Perot can be twice as sensitive as the Michelson, and if dielectric films are used the Fabry–Perot can be as much as four times as sensitive.

The precisions obtained experimentally for the krypton 86 6056 Å and mercury 198 5461 Å lines were in general agreement with the theory, when silver films of different reflectances were used in a Fabry–Perot interferometer in which the plate separations were varied over the range 15 to 225 mm.    Precision curves as a function of $\mu$, obtained by theory and experiment, are similar in form and magnitude.    The optimum precisions in the case of the krypton 86 6056 Å radiation were $2 \cdot 9 \times 10^9$ experimentally and $3 \cdot 7 \times 10^9$ theoretically where the maxima occurred at $\mu = 0 \cdot 25$.    For mercury 198 5461 Å, at $\mu = 0 \cdot 32$ ($t \approx 80$ mm), the corresponding peak precisions were $2 \cdot 5 \times 10^9$ and $5 \cdot 0 \times 10^9$ respectively.    The value of the transmittance of the interferometer ($\mathscr{T}$) was about $0 \cdot 25$ and the scan amplitude and interferometer aperture about $0 \cdot 20$ and $0 \cdot 07$ orders respectively.    Thus, for the krypton 6056 Å line ($w = 0 \cdot 014$ cm$^{-1}$), with $\mu = 0 \cdot 25$, the plate separation is $t = 89$ mm.    The spectral range or wavenumber interval between consecutive orders is $\Delta\sigma = 0 \cdot 056$ cm$^{-1}$.    An amplitude of scan of $0 \cdot 2$ of an order is therefore $0 \cdot 012$ cm$^{-1}$ and an aperture size $b = 0 \cdot 07$ of an order is $0 \cdot 004$ cm$^{-1}$.    Hence in this case most of the line profile is scanned, and about one-half of the profile is " viewed " by the aperture radius $2b$.

The theoretical analysis indicates that these precisions could be improved by a factor of about four if dielectric films ($\mathscr{T} = 0 \cdot 694$) were used, if the scan amplitude was reduced to $0 \cdot 10$ orders, and if the plate separation was reduced to 35 mm for the krypton radiation and 25 mm for the mercury radiation.    An improvement factor of about two would be obtained if silver films, with $\mathscr{T} = 0 \cdot 585$ (best available value), were used.    Thus optimum precisions of $1 \times 10^{10}$ to $2 \times 10^{10}$ are theoretically possible.    By comparison, the best precisions with the Michelson interferometer are $3 \cdot 22 \times 10^9$ and $5 \cdot 64 \times 10^9$ for the krypton 86 and mercury 198

lines respectively. The corresponding optimum plate separations are 107 and
71 mm respectively, and the optimum scan amplitude and interferometer viewing
aperture are 0·32 and 0·20 orders.

With the oscillating Fabry–Perot interferometer it is possible to have
optimum precision for every plate spacing used in wavelength measurement by
choosing the appropriate amplitude of scan of the oscillating plate. For example,
the precision can be held to within 10% of the maximum value for all values of $\mu$
between 0·025 and 0·25. This corresponds to a range in plate separation from
about 10 to 100 mm for the krypton radiation. This is at variance with the static
case in which the flux on the two flanks of the fringe is compared (Hanes 1959).

In the range of reflectivities examined, the optimum precisions for the
Fabry–Perot interferometer are obtained at reflectances of 94, 83, and 73% for
dielectric, silver, and aluminium films respectively. This is also at variance with
Hanes' (1959) conclusions, but is probably due to the use of different transmittance
values for dielectric and aluminium films. The most recent data for these
materials have been used here. The evaluation carried out by Hanes only
considered the photon noise and hence his results should strictly be compared
only with the results shown in Figure 1. However, even if this is done, the above
remarks still apply. Smith (1960) evaluated the limiting precision considering
only the shot noise effect, and the theoretical value which he gives, $5·8 \times 10^9$,
is in reasonable agreement with our results.

There is some evidence that the ratio of the theoretical to the experimental
precisions is smaller for the krypton radiation than for the mercury. This may
be caused by the difference of the discharge conditions. The krypton lamp uses
a d.c. power supply and the mercury power supply is a h.f. unit operating at
100 MHz. The decrease in sensitivity could be due either to inhomogeneities
in the high frequency discharge or to electrical pick-up in the detector circuit.

An assessment of the significance of the theoretical limiting precision of
setting in the measurement of wavelength shifts, or in the comparison of wave-
lengths, must take into account several important experimental factors. First,
an optimum precision of setting of say $2 \times 10^{10}$ for the mercury 198 5461 Å
line using dielectric films with $\mu = 0·10$ orders can only be of use if the detection
system is capable of measuring a fringe shift of about $4·5 \times 10^{-6}$ order. This
would be difficult to achieve in practice and it also implies a very high order of
thermal stability in the interferometer. Secondly, measurement of wavelength
shifts or the comparison of wavelengths always involves a number of pointings
on the fringe patterns. Thirdly, in the comparison of wavelengths, a dielectric
film coating cannot give peak precisions for two wavelengths at the same time.
Further, dielectric films have undesirably high phase dispersion, and, for all
films, phase dispersion must be eliminated by measuring the order of interference
for the two wavelengths at two well-separated path differences. Thus for
wavelength shift measurements at least four pointings are required, and in
wavelength measurements at least six and probably eight pointings, not all of

which can be taken at optimum precision, are necessary. The use of dielectric films for the measurement of small wavelength shifts is satisfactory but, for the comparison of wavelengths, silver films are to be preferred because of their uniform reflectance over a wide wavelength range, their relatively small phase dispersion, and their fairly high transmittance. Realistic values for the maximum precision in measuring wavelength shifts and in the comparison of wavelengths are, therefore, of the order of $9 \cdot 8 \times 10^9$ and $2 \cdot 9 \times 10^9$ respectively where dielectric films are used for the former and silver for the latter.

## VI. Acknowledgments

## VII. Nomenclature

The following symbols are used throughout the paper :

$n$, order of interference,

$n_0$, integral order of interference,

$\delta n$, smallest detectable change in order,

$\tau$, time of observation as a fringe maxima,

$E$, energy of a photon,

$\sigma$, wavenumber of radiation,

$P$, power or radiance of light source,

$t$, plate separation of interferometer,

$T$, transmittance of each interferometer plate,

$R$, reflectance of each interferometer plate,

$\mathscr{T}$, transmittance of interferometer,

$\mathscr{T}_0$, transmittance of optical system,

$D$, diameter of interferometer plates,

$w$, spectral line width in wavenumbers (width at half peak intensity),

$\Delta\sigma$, spectral range (wavenumber interval between two orders),

$\mu$, fraction of an order occupied by line width,

$a$, amplitude of oscillation of interferometer expressed as a fraction of an order,

$b$, radius of viewing aperture in front of photodetector expressed as a fraction of an order,

$\theta$, quantum efficiency of photodetector,

$d\nu$, bandwidth of detecting circuit,

$Q$, quality factor arising from photon noise,

$S$, quality factor arising from shot noise,

$J$, quality factor arising from Johnson noise,

$\Phi$, total noise function,

$\Delta$, interferometer constant.

## VIII. REFERENCES

BELL, D. A. (1960).—" Electrical Noise." 1st Ed. (D. Van Nostrand : London.)

BRUCE, C. F., and HILL, R. M. (1961).—*Aust. J. Phys.* **14** : 64.

ENGELHARD, E. (1958).—*P.V. Com. int. Poids Més.* 2nd Sér. B **26** : 66.

HANES, G. R. (1959).—*Canad. J. Phys.* **37** : 1283.

JONES, R. C. (1958).—*Photogr. Sci. Engng.* **2** : 57.

KREBS, K., and SAUER, A. (1953).—*Ann. Phys. Lpz.* **13** : 359.

LENNIER, R., LAGARDE, D., and FILIPPI, F. (1959).—*Rev. Opt.* **38** (2) : 493.

ROSE, A. (1946).—*J. Soc. Mot. Pict. Engrs.* **47** : 273.

SMITH, D. S. (1960).—*Canad. J. Phys.* **38** : 983.

TERRIEN, J. (1958).—*J. Phys. Radium* **19** : 390.

TROMPETTE, J. (1956).—*J. Phys. Radium* **17** : 124.